Behavioral/Systems/Cognitive

Inactivation of Calcium-Binding Protein Genes Induces 160 Hz Oscillations in the Cerebellar Cortex of Alert Mice

Guy Cheron,[1,2] **David Gall,**[3] **Laurent Servais,**[1,3] **Bernard Dan,**[1,2] **Reinoud Maex,**[4] **and Serge N. Schiffmann**[3]

[1]Laboratory of Electrophysiology, Université Mons-Hainaut, 7000 Mons, Belgium, Laboratories of [2]Movement Biomechanics and [3]Neurophysiology CP601, Université Libre de Bruxelles, 1070 Brussels, Belgium, and [4]Laboratory of Theoretical Neurobiology, University of Antwerp, 2610 Antwerp, Belgium

Oscillations in neuronal populations may either be imposed by intrinsically oscillating pacemakers neurons or emerge from specific attributes of a distributed network of connected neurons. Calretinin and calbindin are two calcium-binding proteins involved in the shaping of intraneuronal Ca^{2+} fluxes. However, although their physiological function has been studied extensively at the level of a single neuron, little is known about their role at the network level. Here we found that null mutations of genes encoding calretinin or calbindin induce 160 Hz local field potential oscillations in the cerebellar cortex of alert mice. These oscillations reached maximum amplitude just beneath the Purkinje cell bodies and are reinforced in the cerebellum of mice deficient in both calretinin and calbindin. Purkinje cells fired simple spikes phase locked to the oscillations and synchronized along the parallel fiber axis. The oscillations reversibly disappeared when gap junctions or either $GABA_A$ or NMDA receptors were blocked. Cutaneous stimulation of the whisker region transiently suppressed the oscillations. However, the intrinsic somatic excitability of Purkinje cells recorded in slice preparation was not significantly altered in mutant mice. Functionally, these results suggest that 160 Hz oscillation emerges from a network mechanism combining synchronization of Purkinje cell assemblies through parallel fiber excitation and the network of coupled interneurons of the molecular layer. These findings demonstrate that subtle genetically induced modifications of Ca^{2+} homeostasis in specific neuron types can alter the observed dynamics of the global network.

Key words: Purkinje cells; fast oscillations; calcium-binding proteins; cerebellum; calretinin; calbindin; targeted gene inactivation

Introduction

Ca^{2+}-binding proteins contribute to shaping presynaptic and postsynaptic signaling (Airaksinen et al., 1997; Edmonds et al., 2000). In the cerebellar cortex, the Ca^{2+}-binding proteins calretinin (Cr) and calbindin (Cb) are expressed in different neurons: Cr in granule cells and Cb in Purkinje cells (PCs) (Résibois and Rogers, 1992). PC activity, the output of the cerebellar cortex, is strongly regulated through the mossy fiber and olivocerebellar systems (Welsh et al., 1995) and through dynamic mechanisms involving intracellular Ca^{2+} fluxes (Llinás and Sugimori, 1980; Llano et al., 1994).

Mice with inactivated Cb or Cr genes ($Cb^{-/-}$ and $Cr^{-/-}$ mice) have impaired motor coordination but no apparent changes in the overall structure of the cerebellar cortex (Airaksinen et al., 1997; Schiffmann et al., 1999). PCs recorded *in vitro* show only modest changes in cellular physiology (Airaksinen et al., 1997; Schiffmann et al., 1999; Barski et al., 2003) (also see Results). *In*

vivo, however, $Cr^{-/-}$ PCs fire simple spikes (SSs) at a dramatically increased rate, probably reflecting the enhanced excitability of their afferent granule cells (Gall et al., 2003). Together with the reduced duration of the complex spike (CS) and the related pause in SS firing (Schiffmann et al., 1999), these changes suggest that influences of the gene defect at the circuit level. It is known that *in vivo* in the cerebral cortex, such enhancement of discharge rates may coexist with oscillatory patterning (Singer, 1999). It has been proposed that spontaneous activity including correlational structures of synchronized oscillations may be useful for the adjustment of the synaptic strength, not only during development (Katz and Shatz, 1996) but in the mature brain as well (McCormick, 1999). Oscillations have been reported in brain areas such as the neocortex and hippocampus in different frequency ranges. Synchronization of oscillation in the γ range (30–70 Hz) between different cortical areas is supposed to underlie the binding of several features into a single perceptual entity (Gray et al., 1989; Singer, 1993). Although the densely reciprocal connecting network of the cerebellar cortex is ideally suited to provide synchronized rhythms (Maex and De Schutter, 1998), the recording of coherent oscillations in cerebellum remains very sparse (Pellerin and Lamarre, 1997; Hartmann and Bower, 1998).

To find out the effect of null mutations of Cr or Cb genes on neural network activity, we recorded, using multiple electrodes, neurons and local field potentials (LFPs) from the cerebellum of $Cr^{-/-}$, $Cb^{-/-}$, and double knock-out $Cb^{-/-}Cr^{-/-}$ mice. Here we report the emergence of spontaneous high-frequency (~160

Hz) oscillations in the cerebellum of these mutant mice. We show that these oscillations result from the on-beam synchronization of PCs, which fire SSs at an increased rate, and demonstrate that they are transiently suppressed by sensorimotor behavior. Pharmacological characterization reveals the dependence of oscillation on gap junctions and GABA$_A$ and NMDA receptor activation. These results support the view that genetically induced modifications of Ca^{2+} homeostasis in granular cells or in PCs trigger the activation of a large network, entraining synchronization of PC assemblies through parallel fiber (PF) excitation and a network of coupled interneurons, providing frequency sharpening through gap junction-mediated synchrony.

Materials and Methods

Control and mutant mice. Sex- and age-matched calbindin-D28K-deficient ($Cb^{-/-}$) (Airaksinen et al., 1997) and calretinin and calbindin-D28K ($Cr^{-/-} Cb^{-/-}$) double knock-out mice (Schiffmann et al., 1999) generated on a mixed 129 × C57BL/6 genetic background were used in all experiments.

Single-unit recording in alert mice. Twenty-four $Cr^{-/-} Cb^{-/-}$, 12 $Cb^{-/-}$, 7 $Cr^{-/-}$, and 10 wild-type (WT) mice (24–35 gm) were prepared for chronic recording of neuronal activity in the cerebellum (Schiffmann et al., 1999). Under general anesthesia induced by xylido–dihydrothiazin (100 mg/kg Rompun; Bayer, Wuppertal, Germany) and ketamine (500 mg/kg Ketalar; Pzifer, Groton, CT), two small bolts were cemented to the skull to immobilize the head during the experimental session. The surface of the uvula of the cerebellum was exposed by reflecting the muscles overlying the cisterna magna, and a small hole was made in the skull. The dura was removed over lobule 9a and 9b and over Crus IIA for whisker-stimulation experiments, and an acrylic recording chamber was constructed around the hole. The recording chamber was maintained covered and in sterile conditions between recording sessions. Animals were kept in accordance with the guidelines established by the ethical committee of Université Mons-Hainaut for the care and use of laboratory animals. Criteria for PC recording and data analysis were the same as those used in a previous study (Schiffmann et al., 1999). Golgi cells were identified using criteria described by Vos et al. (1999). Briefly, the cerebellum was explored with a glass micropipette (1.5–5.0 MΩ impedance). After amplification (1000–2000×) and bandpass filtering (10 Hz to 10 kHz), unit activity was continuously stored on 4 mm digital audio tapes, transferred to a Pentium III personal computer with analog-to-digital converter boards (Power 1401; Cambridge Electronic Design, Cambridge, UK), and treated on-line and off-line by Spike2 CED software (Cambridge Electronic Design). The recorded data were digitized continuously at 10 kHz.

Local field potential analysis. LFPs were analyzed by the wave-triggered average (WTA) technique (Steriade et al., 1998) and the fast Fourier transform algorithm. An oscillation index was computed as peak amplitude divided by total power.

Multiunit recording in alert mice. PC pairs were recorded by means of seven linearly arranged, quartz-insulated, platinum–tungsten fiber microelectrodes with 250 μm interelectrode spacing (Eckhorn and Thomas, 1993). Autocorrelation and cross-correlation histograms with a time bin of 1 msec were plotted for SS firing from single and paired PCs, respectively. The strength of the oscillation was quantified with a rhythm index (RI) introduced by Sugihara et al. (1995). Briefly, peaks and valleys were recognized if their heights and depths exceeded the mean baseline level ± SD (measured at time lags of 250–300 msec). The RI was then defined by the following formula: RI = $a_1/z + b_1/z + a_2/z + b_2/z + \ldots$, in which a_i ($i = 1, 2, \ldots$) is the absolute value of the difference between the height of the ith peak and baseline level, b_i ($i = 1, 2, \ldots$) is the absolute value of the difference between the height of the ith valley and baseline level, and z was the difference between the height of the zero time bin and the baseline level. The synchrony index (SI) was calculated as the area of the central peak on the cross-correlogram and expresses the fraction of synchronous spikes (Maex et al., 2000).

Tactile stimulation of the whisker region. Facial dermatomes of the whisker regions were stimulated by calibrated air puffs delivered by an air pressure system [Picospritzer II (General Valve, Fairfield, NJ)], with an air pressure at the source of the 2.6 bar of 40 psi. Air puffs (20 msec of duration) were applied through a glass pipette (tip diameter, 2 mm). The tip was located 1 cm away from the skin of the whisker region at a lateral angle of 50° with respect to the midline of the head. The timing of air puff stimuli reaching the skin area was determined at the beginning of the recording sessions with a microphone located at the same place as the skin. The microphone signal was full-wave rectified, integrated, and fed into the computer as 1 V rectangular pulses to determine the latency of evoked responses (Gruart et al., 1995). The EMG activity of the zygomaticus major was recorded by bipolar intramuscular electrodes [Teflon-coated stainless-steel wire (diameter, 50 μm)].

In vivo microinjection. Injection micropipettes were filled with a solution of 5 mM bicuculline, 27 mM 2-(3′-carbethoxy-2′-propenyl)-3-amino-6-paramethoxy-phenyl-pyridazinium bromide (SR95531), 6 mM APV, or 48 mM carbenoxolone (a gap junction blocker). Saline solution was injected in control experiments. Injections were performed using an air pressure system (duration, 10 msec; $n = 20$).

To further assess nonspecific effects of carbenoxolone on PC firing, two fiber microelectrodes with 250 μm of interelectrode spacing were adjusted for performing simultaneous but separated records of PC firing and LFP oscillation (LFPO) at the same depth. A micropipette with carbenoxolone was introduced between the two fiber microelectrodes. When PC firing and LFPO were stabilized, carbenoxolone was injected by means of short air pulses (duration, 3 msec; $n = 10$). This latter procedure was used to avoid mechanical effects. Results (see Fig. 7) are expressed as mean ± SD; means are compared by ANOVA test. Student's t tests for dependent samples were also used when appropriate (Statistica 6.0; Statsoft, Tulsa, OK).

Patch-clamp recording. Current-clamp recordings from postnatal day 19 (P19)–P51 PCs were conducted at room temperature using the perforated patch whole-cell configuration of the patch-clamp technique (fast current-clamp mode) (Horn and Marty, 1988). The pipette solution contained the following (in mM): 80 K$_2$SO$_4$, 10 NaCl, 15 glucose, and 5 HEPES, pH adjusted to 7.2 with KOH, and 100 μg/ml nystatin. All recordings were made by using an EPC-8 amplifier (HEKA Elektronik, Lambrecht/Pfalz, Germany) in the fast current-clamp mode in combination with the acquisition software Pulse 8.40 (HEKA Elektronik). The membrane potential was maintained at −80 mV by injecting a steady-state current between 120 and 600 pA. PCs were depolarized by injecting 50 pA current steps (duration, 1 sec). The resulting voltage traces were digitized at 10 kHz with an ITC-16 interface (Instrutech, New York, NY) and analyzed with Igor Pro software (Wavemetrics, Lake Oswego, OR).

Results

Emergence of local field potential oscillations at 160 Hz in mutant mice *in vivo*

Spontaneous LFPOs were found throughout the explored cerebellar regions (vermis, uvula, and nodulus) of alert mutant mice (Fig. 1A). They appeared as spindle-shaped episodes of oscillations (maximal amplitude, 0.54 ± 0.23 mV) with a mean rate of occurrence of 4.5 ± 1.7 episodes per second. LFPOs were recorded in 6 of 7 $Cr^{-/-}$ mice, in 11 of 12 $Cb^{-/-}$ mice, and in all 24 $Cr^{-/-} Cb^{-/-}$ mice, with frequencies of 167.8 ± 36.0, 164.5 ± 36.0, and 164.9 ± 45.3 Hz, respectively. Oscillation indices were significantly higher in $Cr^{-/-} Cb^{-/-}$ (13.9 ± 6.2) than in $Cr^{-/-}$ (6.4 ± 1.8) and $Cb^{-/-}$ (6.7 ± 4.1) mice ($p < 0.001$). LFPOs were present during 40, 50, and 80% of the recording time for $Cr^{-/-}$, $Cb^{-/-}$, and $Cr^{-/-} Cb^{-/-}$ mice, indicating reinforcement of the oscillating state in double knock-out animals. Fast LFPOs were not recorded in WT mice ($n = 10$).

Spatiotemporal mapping of the field potential oscillation

The LFPO amplitude increased when the electrode approached the PC layer, reaching its maximum just beneath the PC bodies (Fig. 1C). In all instances, oscillations recorded in the deep PC
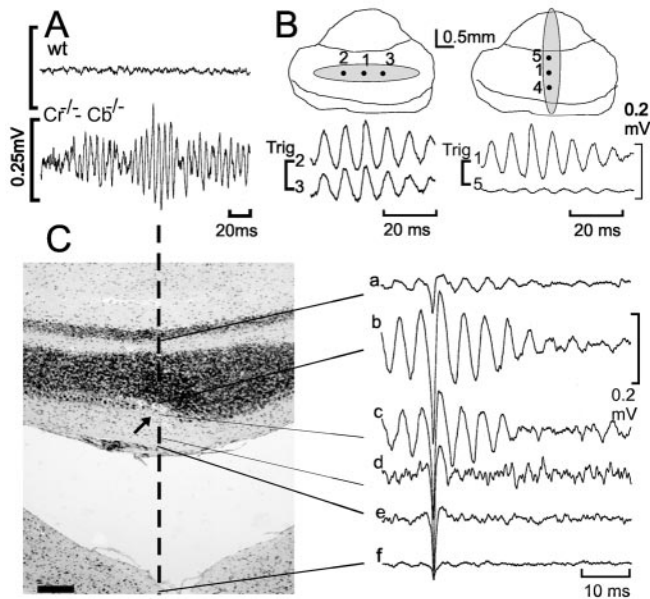
Figure 1. Emergence and spatial coherence of high-frequency oscillations in the cerebellum of $Cr^{-/-}Cb^{-/-}$ mice. *A*, Sample records of LFPOs from wild-type mice (wt; top trace) and $Cr^{-/-}Cb^{-/-}$ mice (bottom trace). *B*, Spatial coherence of LFPOs was analyzed by recording simultaneously from electrodes aligned along the longitudinal [left, tracts 2, 1, 3 (0.5 mm apart)] or rostrocaudal (right, tracts 4, 1, 5) axis of a folium. Pair traces (left), using LFPO recording 2 as a trigger (Trig) for a WTA, show coherent oscillations of the same period and without any significant phase delay, whereas for pair traces (right), using channel 1 as a trigger, no oscillatory pattern was visible. *C*, Depth profile (*Ca–Cf*) of WTA traces throughout the last PC layer of lobule 10 indicates that the maximum amplitude was found just beneath the PC bodies. The arrow indicates an electrolytic lesion at the recording depth of the WTA trace (*Cb*). Scale bar, 0.2 mm. The dashed line represents the recording electrode tract.

Table 1. Purkinje cell firing behavior in alert WT, $Cb^{-/-}$, and $Cb^{-/-}Cr^{-/-}$ mice

Parameter	WT ($n = 35$ cells)	$Cb^{-/-}$ ($n = 78$ cells)	$Cb^{-/-}Cr^{-/-}$ ($n = 150$ cells)
SSf (in Hertz)	41.7 ± 17.5	86.3 ± 45.3*	80.4 ± 44.0*
CSf (in Hertz)	0.42 ± 0.12	0.50 ± 0.22	0.50 ± 0.23
CSd (in milliseconds)	12.3 ± 3.8	6.8 ± 2.2*	6.9 ± 2.4*
Pause (in milliseconds)	24.3 ± 8.0	9.4 ± 6.8*	6.4 ± 6.3*

SSf, Simple spike firing rate; CSf, complex spike firing rate; CSd, complex spike duration. *$p < 0.00001$ compared with age-matched, WT animals; one-way ANOVA.

layer of the nodulus disappeared abruptly when the electrode tip reached the fourth ventricle or the medulla.

Spatial coherence in the coronal plane (i.e., along a PF beam) versus the sagittal plane was measured with multiple electrodes. LFPOs were synchronized at sites along the coronal plane (Fig. 1*B*, left) separated by up to 2 mm (cross-correlation coefficient, 0.91 ± 0.05; $n = 5$). In contrast, paired sites aligned in the sagittal plane (Fig. 1*B*, right) did not show synchronization (−0.03 ± 0.10; $n = 5$).

Firing behavior of individual Purkinje and Golgi cells *in vivo*
Single-unit spike activity of 263 PCs was recorded in $Cb^{-/-}$, $Cb^{-/-}Cr^{-/-}$, and WT alert mice. As summarized in Table 1, the rate of spontaneous SSs was much higher in both mutants than in WT animals. Conversely, the spontaneous rate of CSs was not statistically different. Durations of CSs and of the pauses in SS firing after CSs were significantly reduced. We compared the rhythmicity of SSs in $Cb^{-/-}Cr^{-/-}$ and WT mice by counting the peaks on the autocorrelogram. One-sided peak counts were 0.8 ± 0.1 ($n = 36$) and 6.6 ± 1.5 ($n = 47$) for WT and $Cb^{-/-}Cr^{-/-}$
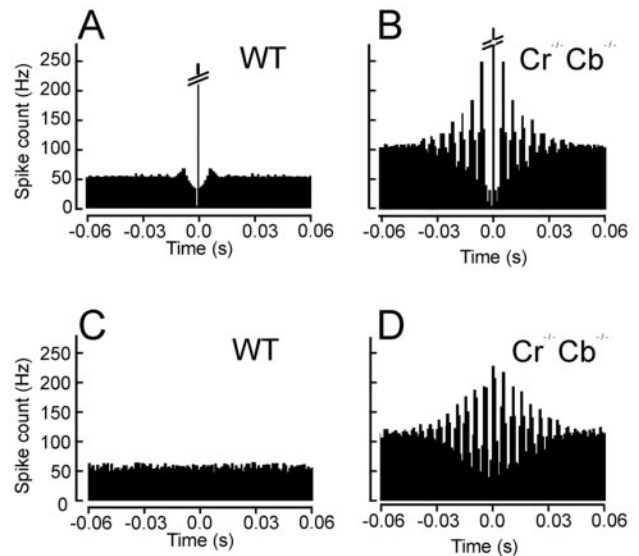

Figure 2. PC rhythmicity in alert WT and in $Cb^{-/-}Cr^{-/-}$ mice. *A, B*, SS autocorrelograms for one representative WT (*A*) and one $Cb^{-/-}Cr^{-/-}$ (*B*) PC demonstrating increased rhythmicity in the mutant. *C, D*, Cross-correlograms of SSs from PC pairs multirecorded along a PF beam (0.5 mm apart) in WT mice (*C*) and $Cb^{-/-}Cr^{-/-}$ mice (*D*), demonstrating PC synchronization in the mutant.

mice, respectively ($p < 0.0001$) (Fig. 2*A,B*). An RI was also significantly higher ($p < 0.0001$) in mutant mice (0.73 ± 0.28) than in WT mice (0.03 ± 0.02).

We compared the discharges of mutant PCs recorded during and in the absence of LFPOs. The SS firing rate was much higher in PCs recorded during LFPOs ($n = 97$) than in PCs recorded in the absence of LFPOs ($n = 131$; 120.6 ± 40.7 vs 54.2 ± 18.4 Hz; $p < 0.00001$). In simultaneous recordings of LFPOs and single PCs, the SS (Fig. 3) and CS (Fig. 4) discharges were phase locked to the LFPOs. SS discharges occurred at the depth of the LFP wave (Fig. 3, top traces), whereas the CS discharge appeared during the LFP ascending phase (Fig. 4).

In contrast, simultaneous recordings of LFPs and Golgi units never demonstrated phase locking between LFP waves and Golgi cell spikes (Fig. 5). However, an increased Golgi cell firing rate was correlated with a significant reduction of concomitant LFPOs. When the interspike interval of Golgi cells decreased to <95 msec, the peak-to-peak amplitude of the LFPO was significantly reduced (Fig. 5).

Synchronization of Purkinje cells along the parallel fiber beam
We recorded 33 coronal PC pairs during LFPOs in four $Cb^{-/-}Cr^{-/-}$ mice to verify whether LFPO synchronization along the PF beam is correlated with synchronous PC firing. All mutant PC pairs showed a significant central peak (SI, 0.24 ± 0.13) on their cross-correlogram and high-frequency oscillations with a number of side peaks of 6.3 ± 1.3 (RI, 3.14 ± 1.45) (Fig. 2*D*). Conversely, in WT mice ($n = 48$ pairs), coronal cross-correlograms were flat in all but three pairs (SI, 0.02 ± 0.05), and high-frequency oscillations were always absent (RI, 0.02 ± 0.09) (Fig. 2*C*).

Effect of peripheral stimuli and motor responses on local field potential oscillations
Given the involvement of PCs in sensorimotor processing (Bower and Woolston, 1983), we stimulated the whisker region
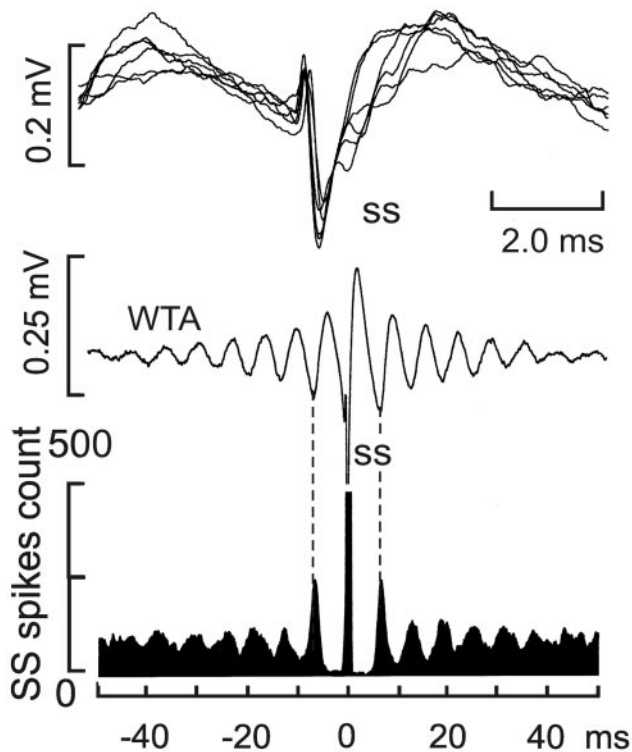
Figure 3. Temporal relationships between LFPOs and PC cell firing. Simultaneous recordings by the same electrode of an isolated PC and a 166 Hz LFPO were made. Shown is the superimposition of single traces ($n = 6$) (top). The WTA of the LFPO using PC SSs as a trigger ($n = 1000$) (middle) is displayed. An SS autocorrelogram, with a central peak truncated (bottom), has the same rhythmicity as the WTA trace. The dashed lines indicate the correspondence between the depth of the first two side waves and the first two side peaks of the SS autocorrelogram.

Figure 4. Temporal relationships between LFPOs and PC cell firing. The same procedure as in Figure 3 was performed with the trigger adjusted on the CS of the same PC. Superimposition of unaveraged traces ($n = 6$) confirmed the recurrent occurrence of the CS in the ascending phase of the LFP oscillation (top). The WTA shows the presence of 166 Hz oscillation around the CS (middle). The SS cross-correlogram has the same rhythmicity as the WTA trace. The dashed lines indicate the correspondence between the depth of the first two side waves and the first two side peaks of the SS autocorrelogram.
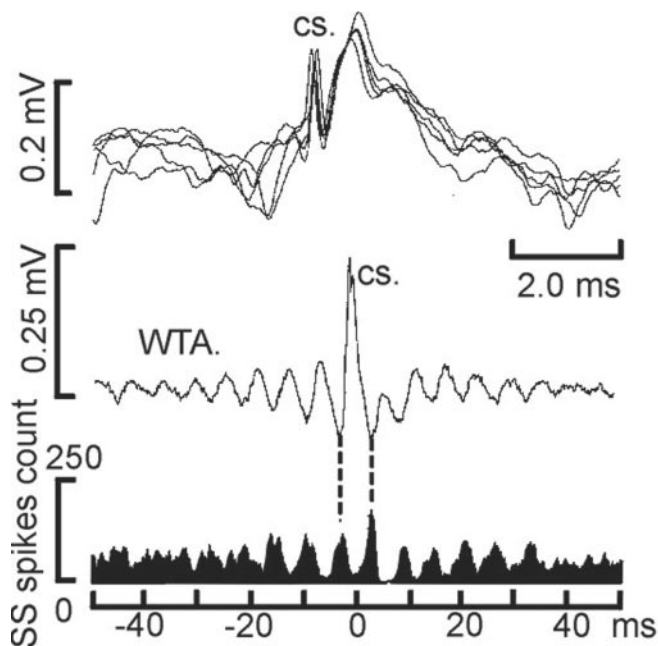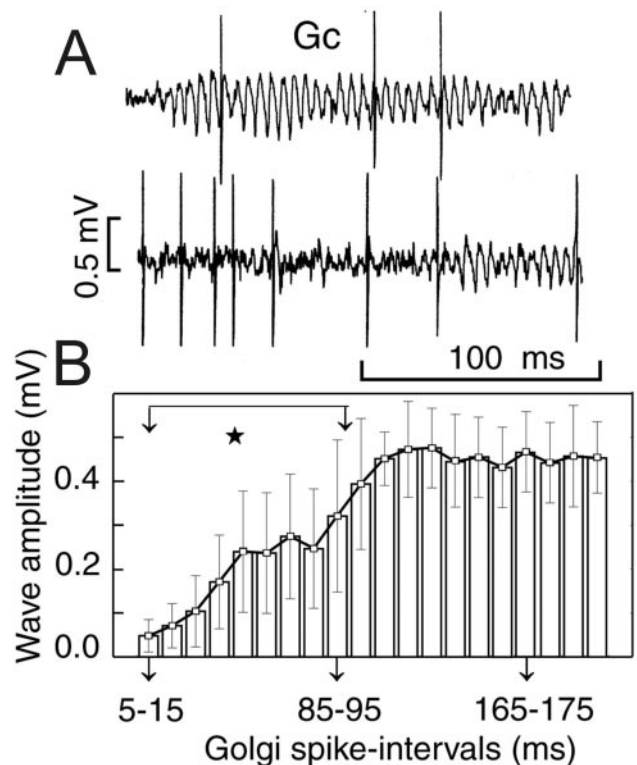

Figure 5. Temporal relationships between LFPOs and Golgi cell (Gc) firing. A, Single trace recordings of Gc spikes and LFPO. B, Quantitative relationship between LFPO amplitude and Gc interspike intervals demonstrates a Gc firing-associated suppression of LFPO (ANOVA; *$p <$ 0.00001). Arrows indicate selected Golgi spike intervals.

and examined the effect on the LFP and a simultaneously recorded PC. Individual PCs ($n = 5$) demonstrated the classical PC responses to cutaneous stimulation characterized by firing rate excitation (Fig. 6C) or inhibition (Fig. 6D) or by transient responses as sequences of inhibition–excitation or excitation–inhibition (Bower and Woolston, 1983). The LFPO was suppressed in response to an air puff on the whiskers, regardless of whether this stimulus caused a facial movement (documented by EMG), but only if the PC also responded to the stimulus (Fig. 6A,B). The LFPO was also suppressed during spontaneous muscle activity but only if the SS firing was also modulated.

Durations of LFPO suppression were 110 ± 42 msec ($n = 13$), 377 ± 241 msec ($n = 66$), and 217 ± 79 msec ($n = 26$) after tactile stimulation without and with a motor response and during spontaneous motor activity, respectively. The duration of the LFPO suppression was strongly correlated ($r = 0.92$) with the duration of the PC response.

Pharmacological properties of local field potential oscillations

To examine which types of synapses contributed to or regulated the LFPOs, we applied blockers of $GABA_A$ and NMDA receptors and of gap junctions. Microinjection of bicuculline ($n = 12$) or SR95531 ($n = 4$), APV ($n = 9$), and carbenoxolone (Draguhn et al., 1998) ($n = 10$) (Fig. 7A,B) reversibly reduced the power of the LFPOs, down to 35.0 ± 17.8, 45.2 ± 17.7, 48.3 ± 20, and 9.5 ± 10.5% of preinjection values, respectively (Fig. 7B).

We ruled out nonspecific actions of carbenoxolone on PC firing ($n = 5$ in two $Cb^{-/-}Cr^{-/-}$ mice) by simultaneously recording LFPs and spikes from single PCs (using separate electrodes) before, during, and after microinjection of carbenox-

olone. One minute after the injection, the LFPO disappeared, whereas the PC firing remained unchanged.

Intrinsic membrane properties of Purkinje cell somata

To determine whether the altered *in vivo* activity resulted from an increased PC excitability, the intrinsic electroresponsiveness of $Cb^{-/-}$ PCs was studied *in vitro*. We measured the SS firing rate at increasing intensities of injected current in slices from five WT and five $Cb^{-/-}$ mice using the perforated-patch whole-cell configuration. The slope of the linear part of these current–frequency plots, which reflects the intrinsic somatic excitability, was not significantly different between WT mice (0.207 ± 0.024 Hz/pA^{-1}) and $Cb^{-/-}$ mice (0.188 ± 0.045 Hz/pA^{-1}). In addition, we did not observe significant modifications in action potential half-width (0.55 ± 0.04 vs 0.59 ± 0.07 msec), resting potential (-64.8 ± 2.2 vs -55.8 ± 4.1 mV), or input resistance (158.5 ± 24.5 vs 212.5 ± 47.9 MΩ).

Discussion

Although *Cr* and *Cb* exhibit a distinct, cell-specific expression in the cerebellar cortex, inactivation of either gene gave rise to increased PC firing rates and spontaneous LFPOs *in vivo*. In $Cr^{-/-}$ mice, the increased PC firing rate and the concomitant LFPOs most likely result from the increased intrinsic excitability of the afferent granule cells (Gall et al., 2003). In addition, PCs of $Cr^{-/-}$ mice have been demonstrated to exhibit a paradoxical calretinin immunoreactivity, probably related to an increase in intracellular Ca^{2+} concentration (Schiffmann et al., 1999).

In $Cb^{-/-}$ mice, no changes in somatic intrinsic PC excitability were found. However, specific alterations in the PC dendritic compartment have been revealed by the detection of increased synaptically evoked Ca^{2+} transients (Airaksinen et al., 1997; Barski et al., 2003) and morphological changes in PC spines (Vecellio et al., 2000). The absence of *Cb* resulted in an increase in various spine parameters of the PC, which were interpreted as a morphological compensation for the lack of soluble calcium buffer in the PC cytoplasm (Vecellio et al., 2000).

Although PCs of WT mice display some rhythmicity in their SS firing pattern (Ebner and Bloedel, 1981; Goossens et al., 2001; Schwarz and Welsh, 2001; present results), this does not give rise to LFPOs. Conversely, in $Cr^{-/-} Cb^{-/-}$ mice, SS rhythmicity was faster, highly amplified, and synchronized along the PF beam. In this case, SS rhythmicity correlated with LFPOs at ~160 Hz. Additional experiments and analyses will examine whether the high-frequency oscillations, which occur spontaneously in knock-out mice, can be evoked in WT mice.

The origin of the high-frequency oscillation

PC populations appear to be the major generator of the 160 Hz LFPO, as suggested by the depth recording profile, the synchro-
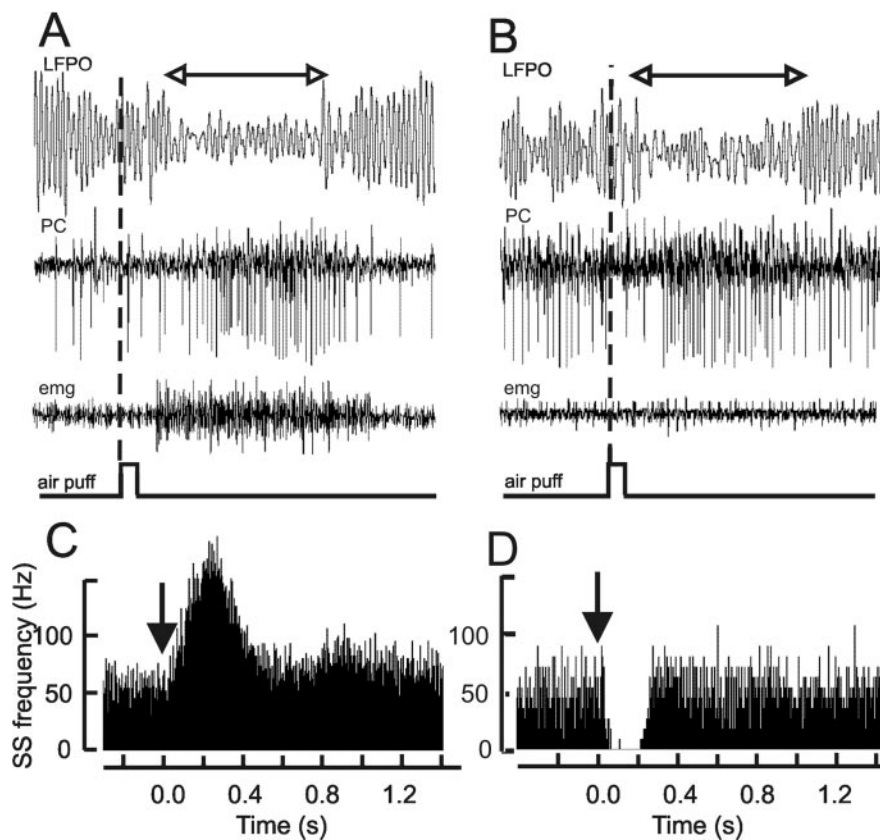

Figure 6. LFPO, PC firing, and EMG responses during cutaneous stimulation of the whisker region. *A, B,* An air puff is produced and evokes suppression of LFPO, PC firing response, and EMG burst (only in *A*). LFPO recording is filtered with a low-pass digital filter (200 Hz). Arrows indicate the extent of LFPO suppression. The dashed lines indicate stimulus onset. *C, D,* Peri-event histograms of SS frequency for two representative PCs excited (*C*) or inhibited (*D*) by air puff stimulation. Arrows indicate stimulus onset.

nization between LFPO and both SSs and CSs, and the LFPO synchronization along the PF beam.

The measured LFPs probably reflect inhibitory synaptic currents in PCs. The highly stereotyped arrangement of closely apposed PCs and their orientation as well as their physiological functioning as an open field make PC assemblies ideal candidates for generating coherent LFPs when their activity is boosted and synchronized. Gradients in synaptic arrangements, with inhibitory synapses mostly located more proximally than parallel fiber synapses, may act as a dipole, generating the largest power close to the plane of PC bodies.

Our experiments with gap junction and GABA$_A$ blockers strongly suggest that the stellate cells likely contribute to the oscillation. In the molecular layer, stellate cells form a densely connected network through fast GABA$_A$ receptor synapses (Kondo and Marty, 1998; Carter and Regehr, 2002) as well as through dendrodendritic gap junctions (Mann-Metzer and Yarom, 1999). This network provides the dominant inhibitory input to PCs through fast GABAergic synapses as well (Puia et al., 1994). In addition, parallel fibers make powerful synapses on stellate cells, with stellate cell firing in response to single afferent input (Carter and Regehr, 2002) favoring synchronization of the oscillations along the folial axis. Moreover, the recent finding that inhibitory and excitatory GABA synapses coexist in the cerebellar interneuron network (Chavas and Marty, 2003) may provide an additional mechanism whereby PC collaterals projecting on molecular interneurons would trigger a rhythmic inhibition–excitation sequence in the coupled interneuron network.
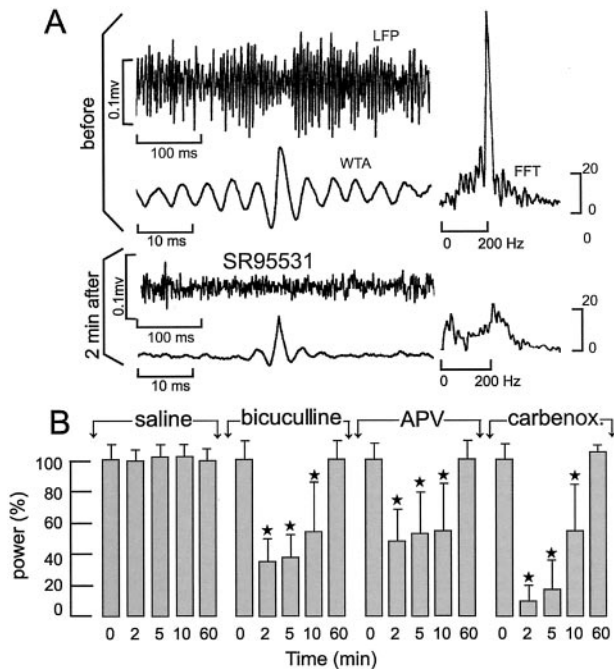
Figure 7. Neuropharmacological regulation of the LFPOs in $Cr^{-/-}Cb^{-/-}$ mice. *A*, Effect of SR95531 on LFPOs. Raw LFP recordings (top), WTA-resulting traces (bottom), and their power spectra (right insets) are shown before and 2 min after the microinjection. FFT, Fast Fourier transform. *B*, Maximal amplitude of the power of the WTA oscillation before and 2, 5, 10, and 60 min after microinjection of saline, bicuculline, APV, and carbenoxolone (carbenox) (values are expressed as a percentage of values before microinjection) (ANOVA; *p < 0.0001).

The LFPOs disappeared immediately when an increased Golgi cell activity suppressed granule cells, reducing the PF input to PCs (Fig. 5B) or when the NMDA receptor-mediated mossy fiber input to granule cells (D'Angelo et al., 1995) was blocked (Fig. 7).

Golgi cells can be excluded as generators of the LFPO, because their firing is not locked to the oscillations. Moreover, the GABA_A receptor synapses they make on granule cells, their principal targets, induce IPSCs with a slow decay (Puia et al., 1994). Finally, because the 160 Hz oscillations are a network phenomenon, we cannot exclude the possibility that types of neurons other than PC and stellate neurons also participate in the rhythm, such as basket cells, the axons of which are electrically interconnected in the "pinceau" ensheathing the initial axon segment of PCs, or Lugaro cells, the myelinated axons of which can span 2 mm along a folium (Dieudonné and Dumoulin, 2000).

Functional significance of gap junctions for the generation of network oscillations
The potent effect of carbenoxolone on this 160 Hz oscillation indicates that a gap junction-coupled network could support its emergence (as demonstrated in the hippocampus) (Draguhn et al., 1998; Traub et al., 1999).

There are at least two possible sites where gap junctions would be able to "sharpen" the 160 Hz LFPO: at the level of stellate and basket cells (Sotelo and Llinás, 1972; Mann-Metzer and Yarom, 1999) and at the level of the axonal plexus of PC collaterals. Several subtypes of connexins [connexin 36 (Teubner et al., 2000; but see Meier et al., 2002), connexin 43 (Simburger et al., 1997), and connexin 47 (Teubner et al., 2001)] are expressed in different neuronal populations in the cerebellum, including molecular interneurons and PCs. However, expression of connexins and

hence the presence of gap junctions in PCs has been called into question recently (Odermatt et al., 2003).

The blocking action of carbenoxolone could switch off the oscillating circuit between molecular interneurons by decreasing the synchronicity inside disinhibition loops. Nonspecific effects of carbenoxolone at the present concentration in vivo are ruled out, because it does not affect the PC firing rate while the concomitant LFPO is suppressed. This is in line with the preservation of antidromically and directly evoked action potentials in the presence of this drug on in vitro preparations (Schmitz et al., 2001).

Physiological role of 160 Hz oscillations
Synchronization of various types of cerebellar neurons has been surmised to underlie the shaping and timing of cerebellar output (Welsh et al., 1995; Maex and De Schutter, 1998; Mann-Metzer and Yarom, 1999; Schwarz and Welsh, 2001), but high-frequency oscillations of local field potential during exploration of the cerebellar cortex with single neuron technology have never been reported in this brain area. However, Adrian (1935) described a 200 Hz potential wave on the surface of the cerebellum. The role of synchrony of parallel fiber inputs to Purkinje cells has been discussed recently as a possible mechanism for this cerebellar rhythm (Isope et al., 2002). However, the analogy between this surface oscillation and the 160 Hz LFPO remains to be investigated. Moreover, intrinsic neuronal Ca^{2+} conductances and intracellular $[Ca^{2+}]$ homeostasis are considered to be crucial partners in the emergence of network activity, including oscillations (Llinás, 1988). Hippocampal oscillations at 200 Hz were recorded in normal rats during sleep or at rest (Buzsáki et al., 1992; Ylinen et al., 1995; Chrobak et al., 2000), indicating that high-frequency oscillations may serve physiological roles when regulated properly. The behavior of the present LFPOs shows similarities with cerebral "resting" rhythmic activities of wakefulness arresting to sensory or motor information, such as α and μ rhythms. μ Oscillations most often occur during a premovement period and cease around movement onset (Donoghue et al., 1998; Ohara et al., 2000; Pfurtscheller et al., 2003). The decrease in μ-oscillation approximately coincides with the increase in γ oscillation above 30 Hz (Pfurtscheller et al., 2003) and with the appearance of firing rate modulation coupled with the motor action (Donoghue et al., 1998). Cortical γ oscillation with different frequency bands has been documented in different areas and their possible functions remain widely debated. For some authors, γ-oscillating activity in the motor system is involved in resetting the descending motor commands needed for changes in motor state (Baker et al., 1999). For others, they represent a neural correlate of attention during demanding sensorimotor behaviors (Murthy and Fetz, 1996). In this context, it was proposed (Fetz et al., 2000) that one functional role could be a global long-term potentiation of synaptic interactions underlying increased attention and motor learning. The relationships between the 160 Hz cerebellar oscillation and the μ- and γ-cortical oscillations need to be studied in freely moving mice.

In the cerebellum, low-frequency oscillations, also inhibited by elicited or spontaneous motor activity, have been described in monkeys and rats, respectively (Pellerin and Lamarre, 1997; Hartmann and Bower, 1998). In such 8–18 Hz oscillations, the granular layer rather than the PC layer was presumed to be the wave generator, and PC firing was never in a clear phasic relationship. In contrast, the phase locking of both SSs and CSs to the present fast oscillation suggests that the high rate and synchronous PC activity, which causes LFPOs, has effects on olivary neu-

rons (Lang et al., 1996) and hence probably also on other cerebellar projection areas (Timofeev and Steriade, 1997).

As in the hippocampus (Draguhn et al., 1998; Moortgat et al., 2000; Traub and Bibbig, 2000; Bartos et al.; 2002; Traub et al., 2002), electrical coupling through gap junctions in the molecular interneurons appears to be involved in PC synchronization. Together, such fast oscillations point to a new mechanism for synchronization that might take part in the coordinating and timing function of the cerebellum (Mauk et al., 2000; Medina et al., 2000).

References

Adrian ED (1935) Discharge frequencies in the central and cerebellar cortex. J Physiol (Lond) 83:33P.

Airaksinen MS, Eilers J, Garaschuk O, Thoenen H, Konnerth A, Meyer M (1997) Ataxia and altered dendritic calcium signaling in mice carrying a targeted null mutation of the calbindin D28k gene. Proc Natl Acad Sci USA 94:1488–1493.

Baker SN, Kilner JM, Pinches EM, Lemon RN (1999) The role of synchrony and oscillations in the motor output. Exp Brain Res 128:109–117.

Barski JJ, Hartmann J, Rose CR, Hoebeek F, Morl K, Noll-Hussong M, De Zeeuw CI, Konnerth A, Meyer M (2003) Calbindin in cerebellar Purkinje cells is a critical determinant of the precision of motor coordination. J Neurosci 23:3469–3477.

Bartos M, Vida I, Frotscher M, Meyer A, Monyer H, Geiger JR, Jonas P (2002) Fast synaptic inhibition promotes synchronized gamma oscillations in hippocampal interneuron networks. Proc Natl Acad Sci USA 99:13222–13227.

Bower JM, Woolston DC (1983) Congruence of spatial organization of tactile projections to granule cell and Purkinje cell layers of cerebellar hemispheres of the albino rat: vertical organization of cerebellar cortex. J Neurophysiol 49:745–766.

Buzsáki G, Horváth Z, Urioste R, Hetke J, Wise K (1992) High-frequency network oscillation in the hippocampus. Science 256:1025–1027.

Carter AG, Regehr WG (2002) Quantal events shape cerebellar interneuron firing. Nat Neurosci 5:1309–1318.

Chavas J, Marty A (2003) Coexistence of excitatory and inhibitory GABA synapses in the cerebellar interneuron network. J Neurosci 23:2019–2031.

Chrobak JJ, Lorincz A, Buzsaki G (2000) Physiological patterns in the hippocampo-entorhinal cortex system. Hippocampus 10:457–465.

D'Angelo E, De Filippi G, Rossi P, Taglietti V (1995) Synaptic excitation of individual rat cerebellar granule cells in situ: evidence for the role of NMDA receptors. J Physiol (Lond) 484:397–413.

Dieudonné S, Dumoulin A (2000) Serotin-driven long-range inhibitory connections in the cerebellar cortex. J Neurosci 20:1837–1848.

Donoghue JP, Sanes JN, Hatsopoulos NG, Gaal G (1998) Neural discharge and local field potential oscillations in primate motor cortex during voluntary movements. J Neurophysiol 79:159–173.

Draguhn A, Traub RD, Schmitz D, Jefferys JGR (1998) Electrical coupling underlies high-frequency oscillations in the hippocampus in vitro. Nature 394:189–192.

Ebner TJ, Bloedel JR (1981) Temporal patterning in simple spike discharge of Purkinje cells and its relationship to climbing fiber activity. J Neurophysiol 45:933–947.

Eckhorn R, Thomas U (1993) A new method for the insertion of multiple microprobes into neural and muscular tissue, including fibre electrodes, fine wires, needles and microsensors. J Neurosci Methods 49:175–179.

Edmonds B, Reyes R, Schwaller B, Roberts WM (2000) Calretinin modifies presynaptic calcium signaling in frog saccular hair cells. Nat Neurosci 3:786–790.

Fetz EE, Chen D, Murthy VN, Matsumura M (2000) Synaptic interactions mediating synchrony and oscillations in primate sensorimotor cortex. J Physiol (Paris) 94:323–331.

Gall D, Roussel C, Susa I, D'Angelo E, Rossi P, Bearzatto B, Galas MC, Blum D, Schurmans S, Schiffmann SN (2003) Altered neuronal excitability in cerebellar granule cells of mice lacking calretinin. J Neurosci 23:9320–9327.

Goossens J, Daniel H, Rancillac A, van der Steen J, Oberdick J, Crepel F, De Zeeuw CI, Frens MA (2001) Expression of protein kinase C inhibitor blocks cerebellar long-term depression without affecting Purkinje cell excitability in alert mice. J Neurosci 21:5813–5823.

Gray CM, Koenig P, Engel AK, Singer W (1989) Stimulus-specific neuronal oscillations in cat visual cortex exhibit inter-columnar synchronization which reflects global stimulus properties. Nature 338:334–337.

Gruart A, Blazquez P, Delgado-Garcia JM (1995) Kinematics of spontaneous, reflex, and conditioned eyelid movements in the alert cat. J Neurophysiol 74:226–248.

Hartmann MJ, Bower JM (1998) Oscillatory activity in the cerebellar hemispheres of unrestrained rats. J Neurophysiol 80:1598–1604.

Horn R, Marty A (1988) Muscarinic activation of ionic currents measured by a new whole-cell recording method. J Gen Physiol 92:145–159.

Isope P, Dieudonné S, Barbour B (2002) Temporal organization of activity in the cerebellar cortex: a manifesto for synchrony. Ann NY Acad Sci 978:164–174.

Katz LC, Shatz CJ (1996) Synaptic activity and the construction of cortical circuits. Science 274:1133–1138.

Kondo S, Marty A (1998) Synaptic currents at individual connections among stellate cells in rat cerebellar slices. J Physiol (Lond) 509:221–232.

Lang EJ, Sugihara I, Llinas R (1996) GABAergic modulation of complex spike activity by the cerebellar nucleoolivary pathway in rat. J Neurophysiol 76:255–275.

Llano I, DiPolo R, Marty A (1994) Calcium-induced calcium release in cerebellar Purkinje cells. Neuron 12:663–673.

Llinás RR (1988) The intrinsic electrophysiological properties of mammalian neurons: insights into central nervous system function. Science 242:1654–1664.

Llinás RR, Sugimori M (1980) Electrophysiological properties of in vitro Purkinje cell somata in mammalian cerebellar slices. J Physiol (Lond) 305:171–195.

Maex R, De Schutter E (1998) Synchronization of Golgi and granule cell firing in a detailed network model of the cerebellar granule cell layer. J Neurophysiol 80:2521–2537.

Maex R, Vos B, De Schutter E (2000) Weak common parallel fibre synapses explain the loose synchrony observed between rat cerebellar Golgi cells. J Physiol (Lond) 523 1:175–192.

Mann-Metzer P, Yarom Y (1999) Electronic coupling interacts with intrinsic properties to generate synchronized activity in cerebellar networks of inhibitory interneurons. J Neurosci 19:3298–3306.

Mauk MD, Medina JF, Nores WL, Ohyama T (2000) Cerebellar function: coordination, learning or timing? Curr Biol 10:522–525.

McCormick DA (1999) Spontaneous activity: signal or noise? Science 23:541–543.

Medina JF, Garcia KS, Nores WL, Taylor NM, Mauk MD (2000) Timing mechanisms in the cerebellum: testing predictions of a large-scale computer simulation. J Neurosci 20:5516–5525.

Meier C, Petrasch-Parwez E, Habbes HW, Teubner B, Guldenagel M, Degen J, Sohl G, Willecke K, Dermietzel R (2002) Immunohistochemical detection of the neuronal connexin36 in the mouse central nervous system in comparison to connexin36-deficient tissues. Histochem Cell Biol 117:461–471.

Moortgat KT, Bullock TH, Sejnowski TJ (2000) Gap junction effects on precision and frequency of a model pacemaker network. J Neurophysiol 83:984–997.

Murthy VN, Fetz EE (1996) Oscillatory activity in sensorimotor cortex of awake monkeys: synchronization of local field potentials and relation to behavior. J Neurophysiol 76:3949–3967.

Odermatt B, Wellershaus K, Wallraff A, Seifert G, Degen J, Euwens C, Fuss B, Bussow H, Schilling K, Steinhauser C, Willecke K (2003) Connexin 47 (Cx47)-deficient mice with enhanced green fluorescent protein reporter gene reveal predominant oligodendrocytic expression of Cx47 and display vacuolized myelin in the CNS. J Neurosci 23:4549–4559.

Ohara S, Ikeda A, Kunieda T, Yazawa S, Baba K, Nagamine T, Taki W, Hashimoto N, Mihara T, Shibasaki H (2000) Movement-related change of electrocorticographic activity in human supplementary motor area proper. Brain 123:1203–1215.

Pellerin JP, Lamarre Y (1997) Local field potential oscillations in primate cerebellar cortex during voluntary movement. J Neurophysiol 78:3502–3507.

Pfurtscheller G, Graimann B, Huggins JE, Levine SP, Schuh LA (2003) Spatiotemporal patterns of beta desynchronization and gamma synchronization in corticographic data during self-paced movement. Clin Neurophysiol 114:1226–1236.

Puia G, Costa E, Vicini S (1994) Functional diversity of GABA-activated

Cl-currents in Purkinje versus granule neurons in rat cerebellar slices. Neuron 12:117–126.

Résibois A, Rogers JH (1992) Calretinin in rat brain: an immunohistochemical study. Neuroscience 46:101–134.

Schiffmann SN, Cheron G, Lohof A, d'Alcantara P, Meyer M, Parmentier M, Schurmans S (1999) Impaired motor coordination and Purkinje cell excitability in mice lacking calretinin. Proc Natl Acad Sci USA 96:5257–5262.

Schmitz D, Schuchmann S, Fisahn A, Draguhn A, Buhl EH, Petrasch-Parwez E, Dermietzel R, Heinemann U, Traub RD (2001) Axo-axonal coupling. A novel mechanism for ultrafast neuronal communication. Neuron 31:831–840.

Schwarz C, Welsh JP (2001) Dynamic modulation of mossy fiber system throughput by inferior olive synchrony: a multielectrode study of cerebellar cortex activated by motor cortex. J Neurophysiol 86:2489–2504.

Simburger E, Stang A, Kremer M, Dermietzel R (1997) Expression of connexin43 mRNA in adult rodent brain. Histochem Cell Biol 107:127–137.

Singer W (1993) Synchronization of cortical activity and its putative role in information processing and learning. Annu Rev Physiol 55:349–374.

Singer W (1999) Neuronal synchrony: a versatile code for the definition of relations? Neuron 24:31–65.

Sotelo C, Llinas R (1972) Specialized membrane junctions between neurons in the vertebrate cerebellar cortex. J Cell Biol 53:271–289.

Steriade M, Amzica F, Neckelmann D, Timofeev I (1998) Spike-wave complexes and fast components of cortically generated seizures. II. Extra- and intracellular patterns. J Neurophysiol 80:1456–1479.

Sugihara I, Lang EJ, Llinas R (1995) Serotonin modulation of inferior olivary oscillations and synchronicity: a multiple-electrode study in the rat cerebellum. Eur J Neurosci 7:521–534.

Teubner B, Degen J, Sohl G, Guldenagel M, Bukauskas FF, Trexler EB, Verselis VK, De Zeeuw CI, Lee CG, Kozak CA, Petrasch-Parwez E, Dermietzel R, Willecke K (2000) Functional expression of the murine connexin 36 gene coding for a neuron-specific gap junctional protein. J Membr Biol 176:249–262.

Teubner B, Odermatt B, Guldenagel M, Sohl G, Degen J, Bukauskas F, Kronengold J, Verselis VK, Jung YT, Kozak CA, Schilling K, Willecke K (2001) Functional expression of the new gap junction gene connexin47 transcribed in mouse brain and spinal cord neurons. J Neurosci 21:1117–1126.

Timofeev I, Steriade M (1997) Fast (mainly 30–100 Hz) oscillations in the cat cerebellothalamic pathway and their synchronization with cortical potentials. J Physiol (Lond) 504:153–168.

Traub RD, Bibbig A (2000) A model of high-frequency ripples in the hippocampus based on synaptic coupling plus axon-axon gap junctions between pyramidal neurons. J Neurosci 20:2086–2093.

Traub RD, Schmitz D, Jefferys JG, Draguhn A (1999) High-frequency population oscillations are predicted to occur in hippocampal pyramidal neuronal networks interconnected by axoaxonal gap junctions. Neuroscience 92:407–426.

Traub RD, Draguhn A, Whittington MA, Baldeweg T, Bibbig A, Bumhl EH, Schmitz D (2002) Axonal gap junctions between principal neurons: a novel source of network oscillations, and perhaps epileptogenesis. Rev Neurosci 13:1–30.

Vecellio M, Schwaller B, Meyer M, Hunziker W, Celio MR (2000) Alterations in Purkinje cell spines of calbindin D-28 k and parvalbumin knockout mice. Eur J Neurosci 12:945–954.

Vos BP, Volny-Luraghi A, De Schutter E (1999) Cerebellar Golgi cells in the rat: receptive fields and timing of responses to facial stimulation. Eur J Neurosci 11:2621–2634.

Welsh JP, Lang EJ, Suglhara I, Llinás RR (1995) Dynamic organization of motor control within the olivocerebellar system. Nature 374:453–457.

Ylinen A, Bragin A, Nadasdy Z, Jando G, Szabo I, Sik A, Buzsaki G (1995) Sharp wave-associated high-frequency oscillation (200 Hz) in the intact hippocampus: network and intracellular mechanisms. J Neurosci 15:30–46.